Stronger temperature-moisture couplings exacerbate the impact of climate warming on global crop yields

Corey Lesk[1,2], Ethan Coffel[3], Jonathan Winter[4], Deepak Ray[5], Jakob Zscheischler[6,7,8], Sonia I. Seneviratne[9], Radley Horton[1]

Affiliations:

[1] Lamont-Doherty Earth Observatory, Palisades, NY, USA

[2] Department of Earth and Environmental Science, Columba University, New York, NY, USA

[3] Department of Geography and the Environment, Syracuse University, Syracuse, NY, USA

[4] Department of Geography, Dartmouth College, Hanover, NH, USA

[5] Institute on the Environment, University of Minnesota, St. Paul, MN, USA

[6] Climate and Environmental Physics, University of Bern, Bern, Switzerland

[7] Oeschger Centre for Climate Change Research, University of Bern, Bern, Switzerland

[8] Department of Computational Hydrosystems, Centre for Environmental Research – UFZ, Leipzig, Germany

[9] Institute for Atmospheric and Climate Science, ETH Zürich, Zürich, Switzerland

Abstract:

Rising air temperatures are a leading risk to global crop production. Recent research has emphasized the critical role of moisture availability in regulating crop responses to heat and the importance of temperature-moisture couplings in driving concurrent heat and drought. Here, we demonstrate that the heat sensitivity of key global crops depends on the local strength of couplings between temperature and moisture in the climate system. Over 1970-2013, maize and soy yields dropped more during hotter growing seasons in places where decreased precipitation and evapotranspiration more strongly accompanied higher temperatures, suggestive of compound heat-drought impacts on crops. Based on this historical pattern and a suite of climate model projections, we show that changes in temperature-moisture couplings in response to warming could enhance the heat sensitivity of these crops as temperatures rise, worsening the impact of warming by -5% (-17 to 11% across climate models) on global average. However, these changes will benefit crops where couplings weaken, including much of Asia, and projected impacts are highly uncertain in some regions. Our results demonstrate that climate change will impact crops not only through warming, but also through changing drivers of compound heat-moisture stresses, which may alter the sensitivity of crop yields to heat as warming proceeds. Robust adaptation of cropping systems will need to consider this underappreciated risk to food production from climate change.

Main:

Introduction

Several studies have identified negative relationships between air temperature and crop yields in observations, signaling the potential for global warming to reduce agricultural output[1–3]. Extreme heat can steeply reduce crop yields both directly through heat stress and indirectly by raising atmospheric vapour demand and contributing to moisture stress[2,4–8]. Because of this dual effect, the impacts of extreme heat are typically amplified by drought, and can be minimized with sufficient soil moisture from either precipitation or irrigation[7,9–16]. Jointly hot and dry conditions thus pose a particular climate risk to global crops, especially under global warming[17].

In many regions, such jointly hot and dry conditions during cropping seasons tend to occur due to physical couplings between temperature and moisture in the climate system[18–20]. These couplings can be conceptualized in two ways: first as a connection between temperature (T) and precipitation (P), and second as a connection between T and evapotranspiration (ET). We refer to the former connection as the *atmospheric circulation* coupling, and the latter as the *land-atmosphere interaction* coupling. While the separability and relative importance of these two couplings is debated[18,21,22] (see Methods), they generally reflect two critical sets of processes that both vary in magnitude over global croplands and strongly influence the local risk of joint heat and drought.

Where the atmospheric circulation coupling is strong, clear skies tend to accompany dry cropping seasons, boosting temperatures at the surface due to increased penetration of solar radiation and delivery of warm compressed air by descending winds[18,20,21,23]. The strength of this coupling is reflected by the magnitude of the negative correlation between temperature and precipitation across years ($r_{T,P} < 0$). Where the land-atmosphere coupling is strong, ET tends to decline during a warmer cropping season, reflected by a negative correlation between T and ET ($r_{T,ET} < 0$). The resulting enhanced sensible heating can further raise air temperatures and atmospheric vapour demand, generating a positive feedback[19,22,24,25]. By contrast, enhanced ET from warmth ($r_{T,ET} > 0$) limits the feedback between warming and drying. Thus, the couplings characterized by negative correlations of T with ET and P drive concurrent and mutually-reinforcing hot and dry conditions during the cropping season in many regions.

Despite the importance of these couplings in controlling the concurrent heat and moisture stresses that so strongly damage crop yields, their effect on global crop responses to current and future temperatures remains a gap in understanding present and future climate impacts on crops. Here, we demonstrate the global influence of temperature-moisture couplings on crop yield sensitivity to temperature over 1970-2013 and project future impacts on crops from changing couplings. We combine historical global yield observations[26,27] with observed and modeled meteorological data to show that during warmer growing seasons, maize and soybean yields drop more steeply where precipitation and ET tend to also decrease. Using simulations from a suite of climate models, we then identify how these couplings are likely to change by the late 21st century. Combining these projections with the historical results, we demonstrate that the modified couplings will likely worsen the impacts of warming on some of the world's most important crops.

Results and Discussion

Historical influence of temperature-moisture couplings on crop heat sensitivity

Over the historical period, we find significant correlations between crop yields and mean seasonal temperature over 20-32% of global maize, soybean, rice and wheat croplands ($p < 0.1$, Fig. 1). While maize and soybean yields generally decline with increasing temperature (by 0.3-0.4 standard deviations (σ) per σ temperature), they benefit from heat over around a quarter of croplands with significant temperature impacts, primarily at higher latitudes and elevations as well as in pockets of the tropics (Fig. 1a-b). Yield benefits from warmer seasons in some locations likely reflect crop limitations by cold and short growing seasons. By contrast, wheat yields are almost universally reduced by higher temperatures in North America and Eurasia (Fig. 1c), likely reflecting the lower physiological heat tolerance of wheat compared to maize[28,29]. While seasonal heat benefits rice yields in parts of Europe and damages them slightly in India, rice yields show a generally weaker connection to temperature (Fig. 1d), as reported elsewhere[1,30]. This may relate to the prevalence of irrigation in rice cropping, which may partially decouple yields from temperature. We also note weak maize yield dependence on temperature where it is mainly irrigated such as northern India, central France, and the western United States (Fig. 1a).

Large portions of the global croplands also experience significant temperature-moisture coupling during the local growing season. Seasonal total precipitation is significantly correlated with mean temperature over 62-89% of cropland ($p < 0.1$, Fig. 1e, Supplementary Fig. 1), with exceptions mainly concentrated in the tropics. These significant interannual correlations are almost entirely negative (>98%), with mean magnitude of -0.5. ET further correlates with temperature over 36-65% of global croplands ($p < 0.1$, Fig. 1f, Supplementary Fig. 1). Correlations are predominantly negative over global croplands but are positive at higher latitudes as well as in southern China (Fig. 1f), a pattern corresponding broadly to moisture- versus energy-limited soil moisture regimes[19], respectively. The majority of global cropland area thus experiences climate couplings whereby lower moisture conditions coincide with higher heat and moisture demand.

We find a global tendency for increasingly negative impacts of temperature on maize and soybean yields with the increasing strength of these temperature-moisture couplings historically. Figure 2 situates the grid-cell yield sensitivity to temperature (presented as the colouring of the points) with respect to the local strength of the two temperature-moisture couplings (presented as the position in the plane of the points). The lower-left quadrant of each panel includes grid cells with both circulation and land-atmosphere couplings ($r_{T,P}$ and $r_{T,ET} < 0$). For maize and soy (Fig. 2a-b), we note that this quadrant contains the bulk of grid cells where yields decline with temperature, with greatest negative yield sensitivities where couplings are strongest. Meanwhile, yields tend to benefit from warmer temperatures where the couplings are weakest ($r_{T,P} \sim 0$ and $r_{T,ET} > 0$).

To quantify these relationships, we regress crop yield sensitivity to temperature on the two couplings and find meaningful global dependence for maize and soy ($r^2 = 0.26$ for maize and 0.43 for soybean, Fig. 2a-b). The regression also affords slope coefficient estimates, $\alpha_{T,P}$ and $\alpha_{T,ET}$, that quantify the steepness of the dependence of yield sensitivity to temperature on the two couplings. On average, yields decline more steeply per σ temperature (slope $\alpha_{T,ET}$ ± standard error = 0.45±0.02 for maize and 0.57±0.02 for soybean, $p < 0.001$) in areas with the most negative $r_{T,ET}$. In other words, crops are around 40% more sensitive to temperature (34% for maize and 43% for soybean) in regions with strong land-atmosphere coupling, compared to where temperature and ET are uncorrelated. The influence of the land-atmosphere coupling on yield sensitivity to temperature is somewhat larger than the influence of circulation coupling on yield sensitivity to temperature (slope $\alpha_{T,P}$ ± standard error = 0.37±0.03 for maize and 0.25±0.04 for soybean, $p < 0.001$). We found no spatial correlation between recent 10-year mean yields (2004-2013) and the two couplings ($r^2 < 0.02$), suggesting that the observed effects are independent of overall crop productivity. Overall, these patterns of higher crop heat sensitivity where couplings are strong is consistent with the compounding of heat impacts on crops by moisture effects where these couplings are strong, and alleviation where they are weak.

By contrast, we find little such dependence on temperature-moisture couplings among the temperature sensitivities of wheat and rice (Fig. 2c-d, $r^2 \leq 0.1$). This may be due in part to the low thermal tolerance of wheat, whose optimal growth temperature is about 10°C cooler than for the other crops[28,29]. Due to its exponential dependence on temperature, atmospheric vapor demand and its impact on crops increase most strongly at relatively high temperatures. However, heat impacts on wheat may be severe at relatively low temperatures, for which atmospheric vapor demand remains relatively low, limiting the scope for compounding of heat impacts by moisture. [31]. For rice, lower heat sensitivity and widespread irrigation may effectively decouple the crop from temperature and moisture (Fig. 1d), similarly precluding compounding impacts[30].

These results suggest that local crop responses to temperature depend not only on crop physiology and temperature stressors, but also on climatological couplings between temperature and moisture. These couplings tend to align heat and moisture stress in time, exposing crops to heat and high atmospheric moisture demand while precipitation and soil moisture are low (Fig. 3). Where the couplings are strong, yields are likely more sensitive to temperature due to antagonistic feedbacks between physiological heat and drought acclimation and stress mechanisms[8,32], notably the impact of stomatal closure on canopy temperature and photosynthesis[8,16,33–37] (Fig. 3). By contrast, where the couplings are weak, heat and high atmospheric moisture demand are more likely to coincide with periods of normal or abundant precipitation and soil moisture, mitigating the impact of heat on crops.

Importantly, these results indicate that the ultimate impact of global warming on some crops will depend not only on the mounting heat hazard itself, but also on the impact of warming on the physical coupling between temperature and moisture. Specifically, they raise the possibility that climate change will affect the sensitivity of crop yields to heat by altering temperature-moisture couplings throughout the world. This potential impact is currently omitted from climate risk projections using statistical models[3,4,6], which assume constant temperature sensitivity into the future, and mechanistic crop models, whose climate projection inputs are typically adjusted to match the historical correlation structure between temperature and moisture[3,38], excluding the potential influence of changes in temperature-moisture couplings.

Impact of projected change in couplings on global crop yields

To examine the implications of these effects for maize and soy under future climate change, we combine the historical dependence of yield sensitivity to temperature on the two couplings (Fig.

2) with simulated future changes in couplings from a suite of 12 CMIP6 global climate models[39]. By 2051-2100 under moderate greenhouse gas emissions (SSP2-4.5), we project substantial changes in $r_{T,ET}$ and to a smaller extent in $r_{T,P}$ (Fig. 4a-b), over much of global croplands in the ensemble median. These changes indicate amplified couplings between temperature and moisture in response to climate warming over croplands in the US, Europe, and southeastern Africa, but reduced couplings across southern to eastern Asia. Based on historical relationships in Fig. 2a-b, these changes in couplings will likely exacerbate yield sensitivity to temperature over a preponderance of croplands, but alleviate it in much of Asia (Fig. 4c).

We project that such heightened crop heat sensitivities due to changing temperature-moisture couplings will worsen the impacts of warming on maize and soy yields across most of the globe (Fig. 5a, Supplementary Fig. 2). In the multi-model median, these additional yield impacts ($\Delta\Delta Y$) amount to regional maize (soy) losses of 7% (9%) in the US, 7% (16%) in western Europe, 12% (24%) in eastern Europe, 9% (5%) in southeastern Africa, and 3% (6%) in southeastern South America, with more modest yield gains of 1% (3%) in eastern Asia (Fig. 5a and d, Supplementary Fig. 2). We note important model uncertainty in these regional figures, which we discuss further below and in Figure 6d. More severe localized yield impacts at sub-regional scales reach ~20% in the United States and ~40% in eastern Europe and southeastern Africa.

These projected additional yield impacts due to changing temperature-moisture couplings ($\Delta\Delta Y$) would add to projected yield losses from warming alone (Fig. 5b), worsening them in some regions (e.g. in central US) but slightly ameliorating them in others (e.g. in eastern Asia, Fig. 5c). In some cool climates such as in the northern US, Canada, and Ukraine, changing couplings may also curtail projected yield gains from warming. Globally, we project that changing couplings will aggravate the impact of warming on maize and soy yields by ~5% relative to recent yields (Fig. 5d, Supplementary Fig. 2), evincing an important but underappreciated risk to agriculture under climate change.

Considerable inter-model variation underlies these multi-model median projections[20]. Over much of global maize croplands, fewer than two-thirds of models agree on the sign of additional yield changes due to coupling responses to warming ($\Delta\Delta Y$, Fig. 6a), especially in the tropics and sub-tropics. Even in areas with high model agreement on sign (mainly in Europe, the US, and eastern Asia), the magnitude of change can vary substantially across models (Fig. 6d, Supplementary Fig. 3). This inter-model variability introduces uncertainty in the projected global mean impacts for the moderate emissions scenario, with model-specific yield impacts ranging from -17 to 11% (Fig. 6b, blue bars).

Alternate emissions scenarios add a further dimension of uncertainty to the projected yield impacts of changing temperature-moisture couplings. Under a high emissions scenario (SSP5-8.5), maize yield losses in the Americas and southeastern Africa are reduced and gains in Asia are increased compared to the moderate emissions scenario (Fig. 6c-d). Surprisingly, these regional responses amount to a global mean *additional* yield gain ($\Delta\Delta Y$) of 1.6% in the ensemble median ('*additional*' in that they only slightly offset large yield loss from warming itself). The counterintuitive non-monotonicity of the global mean response to emissions is ultimately driven by regional coupling changes that alleviate yield sensitivity to temperature, most notably the widespread relative decoupling between T and P under higher emissions (Supplementary Fig. 4). However, we also note large model disagreement in the high emissions scenario, with global mean impacts ranging from -18 to 32% (Fig. 6b, red bars).

The uncertainties in these projections highlight unresolved challenges in simulating temperature-moisture couplings using climate models and their importance to predicting the impact of climate change on global crop production. Specifically, the response of ET (largely mediated by soil and vegetation dynamics and land-atmosphere interaction) and precipitation (largely mediated by regional circulation) to interannual variability in temperature in future climates are both active areas of research[33,40–42]. While some regions with model consensus may reflect predictions with strong physical foundations, such as the enhanced land-atmosphere coupling in Europe with warming[22,43], they may also arise from stronger observational constraints and model validation effort across the northern midlatitudes[20,44]. Some regions lacking model consensus include important breadbaskets in southeast South America and chronically food-insecure and drought-vulnerable southeastern Africa, where weather observations are comparatively sparse and couplings are not well-constrained by observations[20] (Fig. 6, Supplementary Fig. 3). These regions also tend to have the largest differences in estimated historic couplings between CMIP6 and observation-based data (Supplementary Figure 5). Our result show how these uncertainties and potential model inaccuracies presently impede a complete understanding of the risks of climate change to crop production.

Several limitations of our study reflect important challenges and open questions. First, while we assess seasonal-scale yield responses and temperature-moisture couplings, future studies may consider sub-seasonal time scales, particularly the role of the couplings in short-duration heat extremes and flash droughts[43,45], and the differential vulnerability of crop growth stages. Second, we treat crops as passively affected by these couplings, but in some densely-cropped regions they actively influence climate by modifying regional ET[46,47]. While this occurrence is limited to certain high-yielding regions at present, it may become increasingly common with continued crop intensification and thus merits further attention. Third, while we treat circulation and land-atmosphere couplings as distinct, the influence of their overlap and interaction on past and future crop yield sensitivity to temperature should be investigated[18,41]. Fourth, future work should consider the uncertain impact of increased atmospheric CO_2 on future crop responses to combined heat and moisture stresses[48,49], which may weaken or amplify the relationships in Fig. 2 by increasing the water use efficiency of crops (yield per unit water transpired). Finally, further attention to the role of natural vegetation, aerosols, and climate modes such as the El Niño-Southern Oscillation in temperature-moisture couplings is also merited[33,34].

Conclusions

Limitations and uncertainties in the climate models notwithstanding, we draw the following main conclusions from our results. Local heat sensitivity of crop yields depends on the strength of coupling between temperature and moisture for maize and soy, but not for rice and wheat. We propose that this dependence, and its absence for rice and wheat, is consistent with the compounding of heat impacts by moisture stress where couplings are strong, and mitigation where they are weak. By 2051-2100, enhanced couplings over a majority of global cropland will most likely make crops more vulnerable to warming temperatures, with notable exceptions across Asia, where couplings weaken. These climate impacts on crops are widely omitted from climate risk assessments.

Our projections of a mounting threat to crop yields from changing temperature-moisture couplings in a warming climate underscore the need to adapt global crop management and genetics to concurrent heat and moisture stresses. Cropping adaptations, such as breeding for drought and heat tolerance, should thus avoid antagonisms between stress mechanism where couplings strengthen in the future[8,50], but may leverage them where couplings weaken. For instance, irrigation may disrupt the antagonistic feedbacks that lead to compounding heat and moisture stresses, so its effectiveness as a crop adaptation to heat may be enhanced where couplings get stronger in the future. However, the reliability of irrigation may simultaneously decline with strengthening couplings, as drought increasingly limits the availability of water for irrigation during extreme heat (i.e., when it is needed most). As another example, breeding crops for drought tolerance based on stomatal regulation[35,37] or sowing density[51] may exacerbate heat impacts by reducing canopy evaporative cooling or raising crop water demand respectively, a risk that would be less important where couplings weaken (as in much of Asia). Finally, our results may help further calibrate joint temperature-moisture impacts in crop models to assure their usefulness in developing climate-adaptive cropping strategies[14,52].

Efforts to adapt cropping to climates with increasingly strong temperature-moisture couplings may prioritize subsistence cropping areas that are already prone to drought and heat, and where we project enhanced couplings to worsen crop vulnerability in the future. Even with robust adaptations, changes in crop sensitivity to heat under climate change will likely necessitate greater international cooperation in equitable food trade and emergency relief as climate shocks increase.

Methods:

Data and processing

For the historical climate analyses, we combine monthly 0.5° gridded mean temperature and total precipitation observations from the Hadley Center Climate Research Unit (CRU TS4.02)[53] with 0.25° modeled mean temperature and ET data from Global Land Data Assimilation System (GLDAS) Noah land surface model L4, version 2.0[54]. We coarsen the ET data from 0.25° to 0.5°, to match the resolution of the temperature and precipitation data. To represent growing seasonal mean conditions, we average temperature and ET and sum precipitation during the average crop-specific growing periods based on a global crop calendar[55]. For wheat, we define the growing season as three months prior to harvest to exclude the vernalization period for winter wheat. Because ET is the input data with the greatest observational limitations, we verified the robustness of key parameters estimated via the regression model in Equation 2 to three alternative historical ET datasets: 1) GLDAS V2.0 Catchment Land System Model (CLSM) L4 over 1961-2010[54], 2) GLDAS V2.0 Variable Infiltration Capacity (VIC) L4 over 1961-2010[54], and 3) ERA5 Reanalysis over 1980-2010[56].

The crop yield data are based on statistics from ~20,000 subnational political units over 1970-2013, harmonized for consistency with UN Food and Agriculture Organization (FAO) national statistics and gridded to 0.5° resolution[26]. While harmonizing the subnational statistics with national FAO data ensures comparability between nations, it may introduce discontinuities in the data along certain national boundaries, notably Ukraine. We focus on maize, wheat, rice, and soy as crops that are globally dominant in calorie consumption and distributed across the world. For both the climate and crop data, we isolate interannual variability from longer-term trends using singular spectrum analysis (SSA), a non-parametric method that avoids assumptions about the functional form of the climate and yield trends[5,57].

Historical temperature-moisture couplings

To characterize the couplings between temperature and moisture, we compute grid-cell interannual Pearson's correlation coefficients between the detrended temperature and ET from GLDAS for the land-atmosphere coupling ($r_{T,ET}$), and temperature and precipitation from CRU for the circulation coupling ($r_{T,P}$). This approach leverages the strengths of observation-based data for $r_{T,P,}$ but employs model-based data for ET, which is comparatively is sparsely observed over global croplands[20,44]. To improve the robustness of interannual correlations with respect to important modes of climate variability like the El Nino-Southern Oscillation, we use a somewhat longer 50-year time period of 1961-2010 than the study period constrained by the yield data. We define statistical significance of the couplings for each grid-cell using a two-tailed t-test with a threshold of $P < 0.1$.

For clarity, our nomenclature contrasts these two couplings based on the dominant locus of their occurrence either in atmosphere dynamics or land-atmosphere interactions[18,19,21]. However, the two couplings interact physically in some regions and should not be considered strictly distinct[18,21,22]. For instance, global correlations between grid cell $r_{T,ET}$ and $r_{T,P}$ ($r^2 = 0.21$ for maize and 0.29 for soybean) may reflect links among P, ET, and T in the coupled surface-atmosphere system that are not easily disentangled. Despite this, the magnitude of these correlations and the broadly divergent spatial pattern in their historic and projected future magnitude both suggest a prevailing differentiation of the two couplings. For brevity, we present the couplings only for maize in Figure 1 and for the other crops in Supplementary Figure 1, because their spatial pattern does not differ substantially across the different crops.

Historical crop yield sensitivity to heat

We estimate the historical yield sensitivity to temperature as the slope coefficient (β_T) in a simple linear regression model relating detrended yields to temperature for each grid cell:

$$y = \beta_0 + \beta_T T + \varepsilon \qquad (1)$$

where *y* denotes estimated yields, β_0 the intercept, T the mean seasonal temperature, and ε the residual errors. Repeating this analysis for the four crops generates four maps of yield sensitivity to temperature for each crop. We standardize yield and temperature data such that β_T has units of standard deviations of yield per standard deviation of temperature (i.e., is dimensionless). This standardization eases the comparison of yield sensitivity across crop regions with different means and variances of yield and temperature.

The simplicity of this linear model for temperature impacts on yields eases interpretability of the spatial pattern of impacts and the results of subsequent analyses, at the cost of reduced specificity between the impacts of beneficial and detrimental sub-seasonal temperatures that comprise the seasonal mean temperature. Despite this limitation, the spatial pattern and magnitude of estimated yield sensitivity largely agrees with past studies using more complex models. For instance, we compare our unstandardized yield sensitivities aggregated to the national scale with those in the multi-model comparison of Zhao et al. (2018, ref. 4) in Supplementary Figure 8, and find broadly consistent signs and magnitudes for top producing countries for the four crops.

We define statistical significance of the yield sensitivities for each grid cell using a two-tailed t-test with a threshold of $p < 0.1$. Importantly, we do not interpret this yield sensitivity to reflect the response to heat stress alone, but also response of crops to temperature via its impact on vapour pressure deficit, a key variable in moisture stress[2,7,13]. We conduct this analysis for all grid-cells with non-zero crop area to leverage the largest possible diversity of climates and crop systems, regardless their areal intensiveness.

Historical impact of temperature-moisture couplings on yield

Next, we assess the dependence of standardized yield sensitivity to temperature on the two historical coupling measures using a multiple linear regression model of the form:

$$\beta_T = \alpha_0 + \alpha_{T,ET} r_{T,ET} + \alpha_{T,P} r_{T,P} + \varepsilon \quad (2)$$

where $\alpha_{T,ET}$ and $\alpha_{T,P}$ coefficients reflect the response of yield sensitivity to each coupling ($r_{T,ET}$ and $r_{T,P}$), α_0 is the intercept, and ε the residual errors. This method aggregates local yield sensitivities and coupling strengths into a dataset for each crop, and the regression results in two global estimates of the yield sensitivity response to each coupling ($\alpha_{T,ET}$ and $\alpha_{T,P}$) for each crop. Because they represent change in a standardized coefficient per unit change in correlation, $\alpha_{T,ET}$ and $\alpha_{T,P}$ are dimensionless. We include all grid cells with non-zero crop area and significant yield sensitivities to temperature ($p < 0.1$) in this analysis, and note that the regression results are highly robust to a stricter significance threshold of $p < 0.05$ (Supplementary Fig. 9). Based on a minimum threshold for the coefficient of determination (r^2) of 0.2, we judge whether the couplings are substantially predictive of yield sensitivities for each crop, and proceed with future projections only for crops that met this criterion. Variance inflation factors for the models in Equation 2 were 1.2-1.3, indicating low susceptibility of the coefficient estimates to the moderate collinearity between $r_{T,ET}$ and $r_{T,P}$ (r^2 ~0.2-0.3). Estimated model parameters were broadly robust to alternative historical ET datasets, including VIC and CLSM land models from GLDAS and the ERA5 reanalysis (Supplementary Figure 6).

Projecting future change in couplings

To assess future changes in the couplings, we employ projected monthly mean temperature and ET and monthly total precipitation from a suite of Coupled Model Intercomparison Project 6 (CMIP6) general circulation models, run under the SSP2-4.5 moderate emissions scenario[39]. We use all 12 models for which ET data is complete and available. The projected climate data are aggregated to the local growing season. We detrend the seasonal time series using SSA to remove the large influence of long-term forced trends in the climate variables, and regrid the data to a common 0.5° resolution. Despite the lower native resolution of many climate models, we proceed with this higher resolution to conserve the spatial detail of historical mean yields and yield sensitivities to temperature, which are based on higher-resolution data. However, we avoid introducing non-physical results to our downscaled climate projections by using nearest-neighbour approximation rather than interpolating. This method essentially conserves the original model resolution in the climate component of our projections, without sacrificing the higher resolution of observed variables.

To project future changes in the temperature-moisture couplings, we compute $r_{T,ET}$ and $r_{T,P}$ in the climate model data for both the historical period 1961-2010 and a future period of 2051-2100. We select the latter period to be distant enough in the future for climate signals to clearly emerge, but close enough to be useful for adaptation planning. We then compute a multi-model ensemble of correlation change factors by differencing the correlations between the historical and future periods. This differencing approach eliminates extraneous influence of historical mean model biases compared to observations (Supplementary Fig. 5), isolating the relative change in couplings projected by each model relative to its own historical period. Despite this, we note that historical biases likely reflect incomplete model simulation of the processes relevant to change in the couplings. To represent the central tendency of the projection ensemble, we use the multi-model medians of projected change factors in couplings ($\Delta r_{T,ET}$ and $\Delta r_{T,P}$).

Projecting crop yield impacts of changing couplings

We use the historical estimated coefficients relating yield sensitivity to temperature with each coupling ($\alpha_{T,ET}$ and $\alpha_{T,P}$ in equation 2) to project future changes in yield sensitivity to temperature ($\Delta\beta_T$) resulting from changes in the couplings, following:

$$\Delta\beta_T = \alpha_{T,ET}\Delta r_{T,ET} + \alpha_{T,P}\Delta r_{T,P} \qquad (3)$$

This equation employs the regression relation estimated in equation 2, but allows the coupling strength at each grid cell to change based on the climate model projections. The central assumption in this approach is that the future yield sensitivity of each grid cell responds to future changes in the couplings at the global rate dictated by $\alpha_{T,ET}$ and $\alpha_{T,P}$. We note that successful crop adaptation may challenge this assumption (see Conclusions).

To ease the physical interpretation of the projected yield impacts, we convert the projected change in yield sensitivity to dimensional terms using:

$$\Delta B_T = \Delta\beta_T \frac{\sigma_Y}{\sigma_T} \quad (4)$$

where ΔB_T coefficients have units of tons ha^{-1} °C^{-1}. We then project additional yield impacts of warming for each grid cell due to changes in coupling ($\Delta\Delta Y$) by multiplying this coefficient by the multi-model median of the mean seasonal warming by 2051-2100 (ΔT, computed by differencing modeled mean seasonal temperatures between the future and historical periods):

$$\Delta\Delta Y = \Delta B_T \Delta T \quad (5)$$

We present this additional yield impact as a percent of recent local yields averaged over 2004-2013, the 10 most recent years in our dataset, to contextualize the changes relative to local baseline yields. Finally, we average the percent yield changes across all grid cells with significant historical yield sensitivities to estimate net global additional yield impacts due to future changes in temperature-moisture couplings. Note that we map $\Delta r_{T,ET}$, and $\Delta r_{T,P}$ over the full global cropland, regardless of the significance of historical yield sensitivities, to enable interpretation of wider global patterns of change. However, we map $\Delta\Delta Y$ and $\Delta\beta_T$ only where historical yield sensitivity to temperature (β_T) is significant ($P < 0.1$). We also show projected yield change from warming alone to contextualize $\Delta\Delta Y$, however we do not consider these projections themselves to be a methodological improvement on past statistical yield projections using more complex models.

To assess uncertainty across the ensemble of climate models, we recompute equations 3-5 using model-specific changes in the couplings, rather than the ensemble median. We use a consistent multi-model median warming to compute additional yield impact so that the uncertainty analysis isolates differences between model-specific projected changes in couplings, rather than model differences in mean warming. This approach assumes that, at the seasonal scale, the influence of coupling changes on mean warming in each model is small relative to the radiative effect of greenhouse gases and dominant climate feedbacks (e.g. ocean and cloud responses to warming)[43].

We then assess model agreement on the sign of yield change for each grid cell. To do so, we classify whether at least 8 models (2/3 of the ensemble) project either positive change (>10% yield gain), negative change (>10% yield loss), or little change (<10% yield gain or loss). Grid cells where fewer than 8 models agree on the direction of change are classified as areas with substantial model disagreement. We also present histograms of model-specific projected net mean global yield change to reflect the distribution of plausible future global impacts. To account for uncertainty over future emissions, we include in this histogram equivalent results for a high-emissions scenario, SSP5-8.5[39]. We also present $\Delta\Delta Y$ for this scenario to understand the spatial pattern of changes. Finally, we present $\Delta\Delta Y$ for the two emissions scenarios averaged over several regions with noteworthy vulnerability or global importance. The data and methods used in this study are summarized visually in Supplementary Figure 7. Base maps in Figures 1 and 4-6 are developed by Generic Mapping Tools and used under a creative commons license.

Code availability: The processing and analysis codes are available from: https://github.com/clesk/couplings-heat-crops

Data availability: Datasets supporting the results of this paper are freely available from the references and links listed in Supplementary Table 1. Crop yield data are available from D. R. upon request. The intermediate datasets are available at: https://github.com/clesk/couplings-heat-crops

References

1. Lobell, D. B. & Field, C. B. Global scale climate – crop yield relationships and the impacts of recent warming. *Environ. Res. Lett.* **2**, (2007).
2. Lobell, D. B. *et al.* The critical role of extreme heat for maize production in the United States. *Nat. Clim. Chang.* **3**, 497–501 (2013).
3. Zhao, C. *et al.* Temperature increase reduces global yields of major crops in four independent estimates. *Proc. Natl. Acad. Sci.* **114**, 1–6 (2017).
4. Schlenker, W. & Roberts, M. J. Nonlinear temperature effects indicate severe damages to U.S. crop yields under climate change. *Proc. Natl. Acad. Sci.* **106**, 15594–15598 (2009).
5. Vogel, E. *et al.* The effects of climate extremes on global agricultural yields. *Environ. Res. Lett.* **14**, 054010 (2019).
6. Lobell, D. B., Bänziger, M., Magorokosho, C. & Vivek, B. Nonlinear heat effects on African maize as evidenced by historical yield trials. *Nat. Clim. Chang.* **1**, 42–45 (2011).
7. Urban, D. W., Sheffield, J. & Lobell, D. B. The impacts of future climate and carbon dioxide changes on the average and variability of US maize yields under two emission scenarios. *Environ. Res. Lett.* **10**, (2015).
8. Prasad, P. V. V. *et al.* Impacts of Drought and/or Heat Stress on Physiological, Developmental, Growth, and Yield Processes of Crop Plants. R*esponse of crops to limited water: Understanding and modeling water stress effects on plant growth processes*, 301–356 (2008) doi:10.2134/advagricsystmodel1.c11.
9. Troy, T. J., Kipgen, C. & Pal, I. The impact of climate extremes and irrigation on US crop yields. *Environ. Res. Lett.* **10**, (2015).
10. Carter, E. K., Melkonian, J., Riha, S. J. & Shaw, S. B. Separating heat stress from moisture stress : analyzing yield response to high temperature in irrigated maize. *Environ. Res. Lett* **11**(9), 094012 (2016
11. Matiu, M., Ankerst, D. P. & Menzel, A. Interactions between temperature and drought in global and regional crop yield variability during 1961-2014. *PLoS One* **12**, 1–23 (2017).
12. Coffel, E. D. *et al.* Future Hot and Dry Years Worsen Nile Basin Water Scarcity Despite Projected Precipitation Increases. *Earth's Futur.* **7**, 967–977 (2019).
13. Rigden, A. J., Mueller, N. D., Holbrook, N. M., Pillai, N. & Huybers, P. Combined influence of soil moisture and atmospheric evaporative demand is important for accurately predicting US maize yields. *Nat. Food* **1**, (2020).
14. Schauberger, B. *et al.* Consistent negative response of US crops to high temperatures in observations and crop models. *Nat. Commun.* **8**, (2017).
15. Ortiz-Bobea, A., Wang, H., Carrillo, C. M. & Ault, T. R. Unpacking the climatic drivers of US agricultural yields. *Environ. Res. Lett.* **14**, (2019).
16. Siebert, S., Webber, H., Zhao, G. & Ewert, F. Heat stress is overestimated in climate impact studies for irrigated agriculture. *Environ. Res. Lett.* **12**, 0–4 (2017).
17. Lesk, C. & Anderson, W. Decadal variability modulates trends in concurrent heat and drought over global croplands. *Environ. Res. Lett.* (2021).

18. Berg, A. *et al.* Interannual coupling between summertime surface temperature and precipitation over land: Processes and implications for climate change. *J. Clim.* **28**, 1308–1328 (2015).

19. Seneviratne, S. I. *et al.* Investigating soil moisture-climate interactions in a changing climate: A review. *Earth-Science Rev.* **99**, 125–161 (2010).

20. Zscheischler, J. & Seneviratne, S. I. Dependence of drivers affects risks associated with compound events. *Sci. Adv.* **3**, 1–11 (2017).

21. Trenberth, K. E. & Shea, D. J. Relationships between precipitation and surface temperature. *Geophys. Res. Lett.* **32**, 1–4 (2005).

22. Seneviratne, S. I., Lüthi, D., Litschi, M. & Schär, C. Land-atmosphere coupling and climate change in Europe. *Nature* **443**, 205–209 (2006).

23. Horton, R. M., Mankin, J. S., Lesk, C., Coffel, E. & Raymond, C. A Review of Recent Advances in Research on Extreme Heat Events. *Curr. Clim. Chang. Reports* **2**, 242–259 (2016).

24. Berg, A. *et al.* Impact of soil moisture-atmosphere interactions on surface temperature distribution. *J. Clim.* **27**, 7976–7993 (2014).

25. Miralles, D. G., Teuling, A. J., Van Heerwaarden, C. C. & De Arellano, J. V. G. Mega-heatwave temperatures due to combined soil desiccation and atmospheric heat accumulation. *Nat. Geosci.* **7**, 345–349 (2014).

26. Ray, D. K. *et al.* Climate change has likely already affected global food production. *PLoS One* **14**, 1–18 (2019).

27. Ray, D. K., Gerber, J. S., Macdonald, G. K. & West, P. C. Climate variation explains a third of global crop yield variability. *Nat. Commun.* **6**, 1–9 (2015).

28. Liu, B. *et al.* Similar estimates of temperature impacts on global wheat yield by three independent methods. *Nat. Clim. Chang.* **6**, 1130–1136 (2016).

29. Sánchez, B., Rasmussen, A. & Porter, J. R. Temperatures and the growth and development of maize and rice: A review. *Glob. Chang. Biol.* **20**, 408–417 (2014).

30. Welch, J. R. *et al.* Rice yields in tropical/subtropical Asia exhibit large but opposing sensitivities to minimum and maximum temperatures. *Proc. Natl. Acad. Sci. U. S. A.* **107**, 14562–14567 (2010).

31. Zhang, T., Lin, X. & Sassenrath, G. F. Current irrigation practices in the central United States reduce drought and extreme heat impacts for maize and soybean, but not for wheat. *Sci. Total Environ.* **508**, 331–342 (2015).

32. Mittler, R. Abiotic stress, the field environment and stress combination. Trends in plant science, **11**(1), 15-19, (2006).

33. Swann, A. L. S. Plants and Drought in a Changing Climate. *Curr. Clim. Chang. Reports* **4**, 192–201 (2018).

34. Skinner, C. B., Poulsen, C. J. & Mankin, J. S. Amplification of heat extremes by plant CO2 physiological forcing. *Nat. Commun.* **9**, 1–11 (2018).

35. Gates, D. M. Transpiration and leaf temperature. *Annu. Rev. Plant. Physiol.* **19**, 211–238

(1968).

36. Crafts-Brandner, S. J. & Salvucci, M. E. Sensitivity of photosynthesis in a C4 plant, maize, to heat stress. *Plant Physiol.* **129**, 1773–1780 (2002).

37. Grossiord, C. *et al.* Plant responses to rising vapor pressure deficit. *New Phytol.* **226**, 1550–1566 (2020).

38. Rosenzweig, C. *et al.* Assessing agricultural risks of climate change in the 21st century in a global gridded crop model intercomparison. *Proc. Natl. Acad. Sci.* **111**, 3268–3273 (2014).

39. Eyring, V. *et al.* Overview of the Coupled Model Intercomparison Project Phase 6 (CMIP6) experimental design and organization. *Geosci. Model Dev.* **9**, 1937–1958 (2016).

40. Seth, A. *et al.* Monsoon Responses to Climate Changes—Connecting Past, Present and Future. *Curr. Clim. Chang. Reports* 63–79 (2019) doi:10.1007/s40641-019-00125-y.

41. Orlowsky, B. & Seneviratne, S. I. Statistical analyses of land-atmosphere feedbacks and their possible pitfalls. *J. Clim.* **23**, 3918–3932 (2010).

42. Lesk, C., Coffel, E. & Horton, R. Net benefits to US soy and maize yields from intensifying hourly rainfall. *Nat. Clim. Chang.* **10**, 819–822 (2020).

43. Vogel, M. M. *et al.* Regional amplification of projected changes in extreme temperatures strongly controlled by soil moisture-temperature feedbacks. *Geophys. Res. Lett.* **44**, 1511–1519 (2017).

44. Mueller, B. *et al.* Evaluation of global observations-based evapotranspiration datasets and IPCC AR4 simulations. *Geophys. Res. Lett.* **38**, 1–7 (2011).

45. Pendergrass, A. G. *et al.* Flash droughts present a new challenge for subseasonal-to-seasonal prediction. *Nat. Clim. Chang.* **10**, 191–199 (2020).

46. Mueller, N. D. *et al.* Global relationships between cropland intensification and summer temperature extremes over the last 50 years. *J. Clim.* **30**, 7505–7528 (2017).

47. He, Y., Lee, E. & Mankin, J. S. Seasonal tropospheric cooling in Northeast China associated with cropland expansion. *Environ. Res. Lett.* **15**, (2020).

48. Ainsworth, E. A. & Long, S. P. 30 years of free-air carbon dioxide enrichment (FACE): What have we learned about future crop productivity and its potential for adaptation? *Glob. Chang. Biol.* **27**, 27–49 (2021).

49. Deryng, D. *et al.* Regional disparities in the beneficial effects of rising CO2 concentrations on crop water productivity. *Nat. Clim. Chang.* **6**, 786–790 (2016).

50. Challinor, A. J., Koehler, A.-K., Ramirez-Villegas, J., Whitfield, S. & Das, B. Current warming will reduce yields unless maize breeding and seed systems adapt immediately. *Nat. Clim. Chang.* **6**, 954–958 (2016).

51. Lobell, D. B., Deines, J. M. & Tommaso, S. Di. Changes in the drought sensitivity of US maize yields. *Nat. Food* **1**, 729–735 (2020).

52. Bassu, S. *et al.* How do various maize crop models vary in their responses to climate change factors? *Glob. Chang. Biol.* **20**, 2301–2320 (2014).

53. Harris, I., Jones, P. D., Osborn, T. J. & Lister, D. H. Updated high-resolution grids of monthly climatic observations – the CRU TS3.10 dataset. *Int. J. Clim.* **34**, 623–642 (2014).

54. Rodell, M. *et al.* The Global Land Data Assimilation System. *Bull. Am. Meteorol. Soc.* **85**, 381–394 (2004).

55. Sacks, W. J., Deryng, D. & Foley, J. A. Crop planting dates : an analysis of global patterns. *Glob. Ecol. Biogeogr.* **19**, 607–620 (2010).

56. Hersbach, H. *et al.* The ERA5 global reanalysis. *Q. J. R. Meteorol. Soc.* **146**, 1999–2049 (2020).

57. Vautard, R., Yiou, P. & Ghil, M. Singular-spectrum analysis: A toolkit for short, noisy chaotic signals. *Phys. D Nonlinear Phenom.* **58**, 95–126 (1992).

Materials and Correspondence: Correspondence to Corey Lesk (lesk@ldeo.columbia.edu)

Acknowledgments: This material is based upon work supported by the National Science Foundation Graduate Research Fellowship under Grant No. DGE – 1644869. JW was supported by the National Science Foundation under Grant No. BCS – 184018. JZ acknowledges the Swiss National Science Foundation (Ambizione grant 179876) and the Helmholtz Initiative and Networking Fund (Young Investigator Group COMPOUNDX, grant agreement VH-NG-1537). SIS acknowledges support from the European Union’s Horizon 2020 Research and Innovation Program (grant agreement 821003 (4C)) and the Swiss National Foundation in relation to the DAMOCLES COST Action (project “Compound events in a changing climate”). Thanks are due to Jonas Jägermeyr, Justin Mankin, Ruth DeFries, and Mingfang Ting for constructive feedback on methods and results. We acknowledge the World Climate Research Programme, which, through its Working Group on Coupled Modelling, coordinated CMIP6. We thank the climate modeling groups for producing and making available their model output, the Earth System Grid Federation (ESGF) for archiving the data, and the funding agencies who support CMIP6 and ESGF.

Author contributions: C.L., E.C., and J.M.W designed and coordinated this research. C.L. conducted the analysis. All authors discussed the methods and results and wrote the manuscript.

Competing interests: Authors declare no competing interests.

Figure Captions:

Figure 1: Crop yield sensitivity to temperature and temperature-moisture couplings across global croplands. Standardized yield sensitivity to mean growing season maximum air temperature estimated as the linear slope coefficient, with units of standard deviations (σ) of yield per σ temperature, for a) maize, b) soybean, c) wheat, and d) rice. Yield and temperature observational data are detrended to remove long-term warming and yield trends. Stippling denotes significant slope coefficients (two-tailed $p < 0.1$, t-test). Land area without crops is shown in gray. e) Circulation coupling strength, measured as the interannual correlation between detrended observed growing season mean temperature and total precipitation ($r_{T,P}$). f) Land-atmosphere coupling, measured as the interannual correlation between detrended modeled growing season mean temperature and evapotranspiration ($r_{T,ET}$). Couplings in e-f are shown for the maize growing season and over the full global cropland where data is available to ease interpretation of global patterns. Couplings for other growing seasons are shown in Supplementary Fig. 1.

Figure 2: Global dependence of yield sensitivity to temperature on two temperature-moisture couplings. Estimated standardized yield sensitivity to mean growing season maximum air temperature (colouring of points) plotted in relation to correlations of temperature with ET (land-atmosphere coupling, vertical axes) and precipitation (circulation coupling, horizontal axes), for a) maize (n = 4,771 grid cells), b) soybean (n = 2,663), c) wheat (n = 5,062), and d) rice (n = 2,800). Each data point represents one grid cell. Data are shown for areas with significant yield response to temperature (two-tailed $p < 0.1$). Slope coefficients relating yield sensitivity to each coupling ($\alpha_{T,P}$ and $\alpha_{T,ET}$) are annotated on their respective axes. Reported multiple r^2 values are for the multiple regression model relating yield sensitivity to the two couplings.

Figure 3: Schematic of potential mechanism for compound heat and moisture impacts on crops in regions with strong temperature-moisture couplings. Where temperature-moisture couplings are strong, hot growing seasons are more likely to be also dry, depicted by the sun at upper left. Ensuing effects of consequence to crops that are linked to strong circulation coupling ($r_{T,P} < 0$) are shown in the blue square at left, while effects linked to strong land-atmosphere coupling ($r_{T,ET} < 0$) are shown in the yellow square at right. Red arrows show antagonistic feedbacks by which correlations of temperature with P and ET can induce compounding heat and moisture stresses on crops.

Figure 4: Projected future changes in temperature moisture couplings and yield sensitivity to temperature in response to warming. a) Projected change in circulation coupling (detrended interannual $r_{T,P}$) over 2051-2100 under a moderate emissions scenario (SSP2-4.5), compared to historical couplings over 1961-2010. The median of an ensemble of 12 CMIP6 climate model projections is shown for each grid cell. b) Same as a), but for land-atmosphere coupling ($r_{T,ET}$). c) Projected change in standardized maize yield sensitivity to temperature in response to changes in the two couplings, based on global slope coefficients from in Fig. 2a. For a-b) projections are shown over the full global maize croplands to facilitate

interpretation of broader patterns, while for c) projections are shown only for areas with significant historical maize yield sensitivity to temperature ($p < 0.1$); gray shading shows croplands with insignificant yield dependence on temperature.

Figure 5: Projected additional impact of future warming on maize yields due to changing temperature-moisture couplings. a) Ensemble median additional impact of warming on maize yields from projected changes in $r_{T,ET}$ and $r_{T,P}$ over 2051-2100 under a moderate emissions scenario (SSP2-4.5), as a percent of local mean of recent yields (2004-2013). b) Maize yield changes (as a percent of recent yield) from ensemble median warming only, projected using historical yield sensitivity to temperature from Fig. 1a. c) Projected total yield impacts, estimated as the sum of impacts from changing couplings and warming only (note that the scale differs from a-b). Projections in a-c) are shown only for areas with significant historical maize yield sensitivity to temperature ($p < 0.1$); gray shading shows croplands with insignificant yield dependence on temperature. d) Yield impacts averaged across selected key regions and globally. Model uncertainties associated with these ensemble median results are shown in Figure 6

Figure 6: Uncertainty in projected additional maize yield impact due to changing temperature-moisture couplings. a) Model agreement on local sign of projected additional yield impact due to changing temperature-moisture couplings ($\Delta\Delta Y$) under a moderate emissions scenario by 2051-2100. Colouring denotes areas where at least two-thirds (8 out of 12) of the models in the ensemble agree on either positive (blue), negative (brown), or no substantial change (within +/-10%, beige). Grey denotes areas with less than two-thirds model agreement on direction of change. b) Distribution of model-specific global mean additional yield impact due to changing couplings ($\Delta\Delta Y$) for the moderate emissions (SSP2-4.5, blue) and high emissions (SSP5-8.5, red) scenarios. Vertical red and blue lines denote multi-model median global mean impacts. Additional yield impacts are expressed as a percentage of 2004-2013 mean yields, averaged over areas with significant temperature effects on yield (Fig. 1a). c) Ensemble median additional impact of warming on maize yields due to changes in couplings over 2051-2100 under the high emissions scenario (SSP5-8.5), as a percent of local mean of recent yields (2004-2013). Projections are shown only for areas with significant historical maize yield sensitivity to temperature ($P < 0.1$); gray shading shows croplands with insignificant yield dependence on temperature. d) Same as b), but with additional yield impacts averaged over selected regions. Boxplot centerline denotes multi-model median; whiskers, tail projections within 1.5 interquartile range; and points, outlier projections.

,

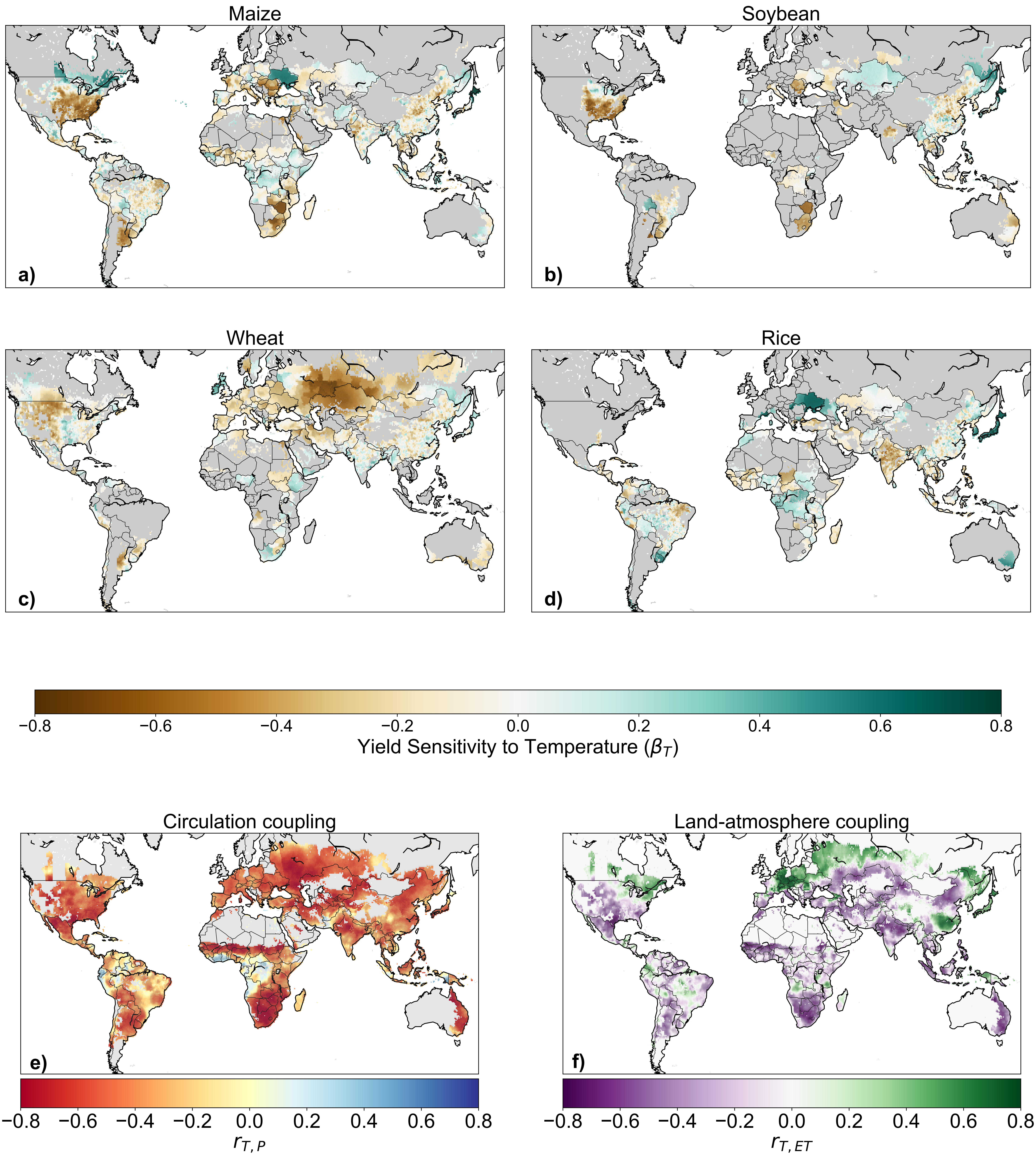
Maize
Soybean
a)
b)
Wheat
Rice
c)
d)
−0.8
−0.6
−0.4
−0.2
0.0
0.2
0.4
0.6
0.8
Yield Sensitivity to Temperature (β_T)
Circulation coupling
Land-atmosphere coupling
e)
f)
−0.8
−0.6
−0.4
−0.2
0.0
0.2
0.4
0.6
0.8
$r_{T,P}$
−0.8
−0.6
−0.4
−0.2
0.0
0.2
0.4
0.6
0.8
$r_{T,ET}$

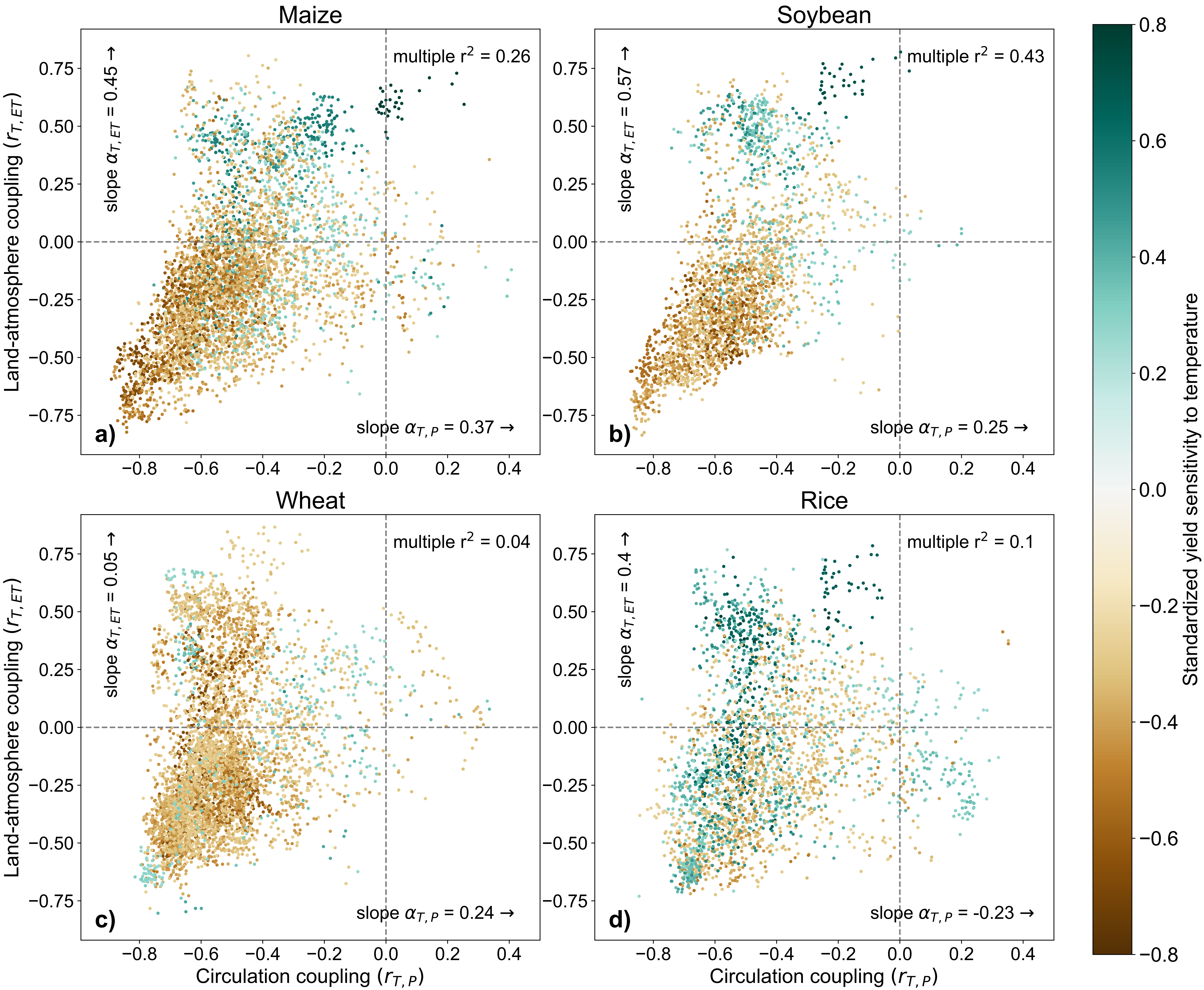
Maize
Soybean
Wheat
Rice
multiple r^2 = 0.26
multiple r^2 = 0.43
multiple r^2 = 0.04
multiple r^2 = 0.1
slope $\alpha_{T,ET}$ = 0.45 →
slope $\alpha_{T,ET}$ = 0.57 →
slope $\alpha_{T,ET}$ = 0.05 →
slope $\alpha_{T,ET}$ = 0.4 →
slope $\alpha_{T,P}$ = 0.37 →
slope $\alpha_{T,P}$ = 0.25 →
slope $\alpha_{T,P}$ = 0.24 →
slope $\alpha_{T,P}$ = -0.23 →
a)
b)
c)
d)
Land-atmosphere coupling ($r_{T,ET}$)
Circulation coupling ($r_{T,P}$)
Standardized yield sensitivity to temperature

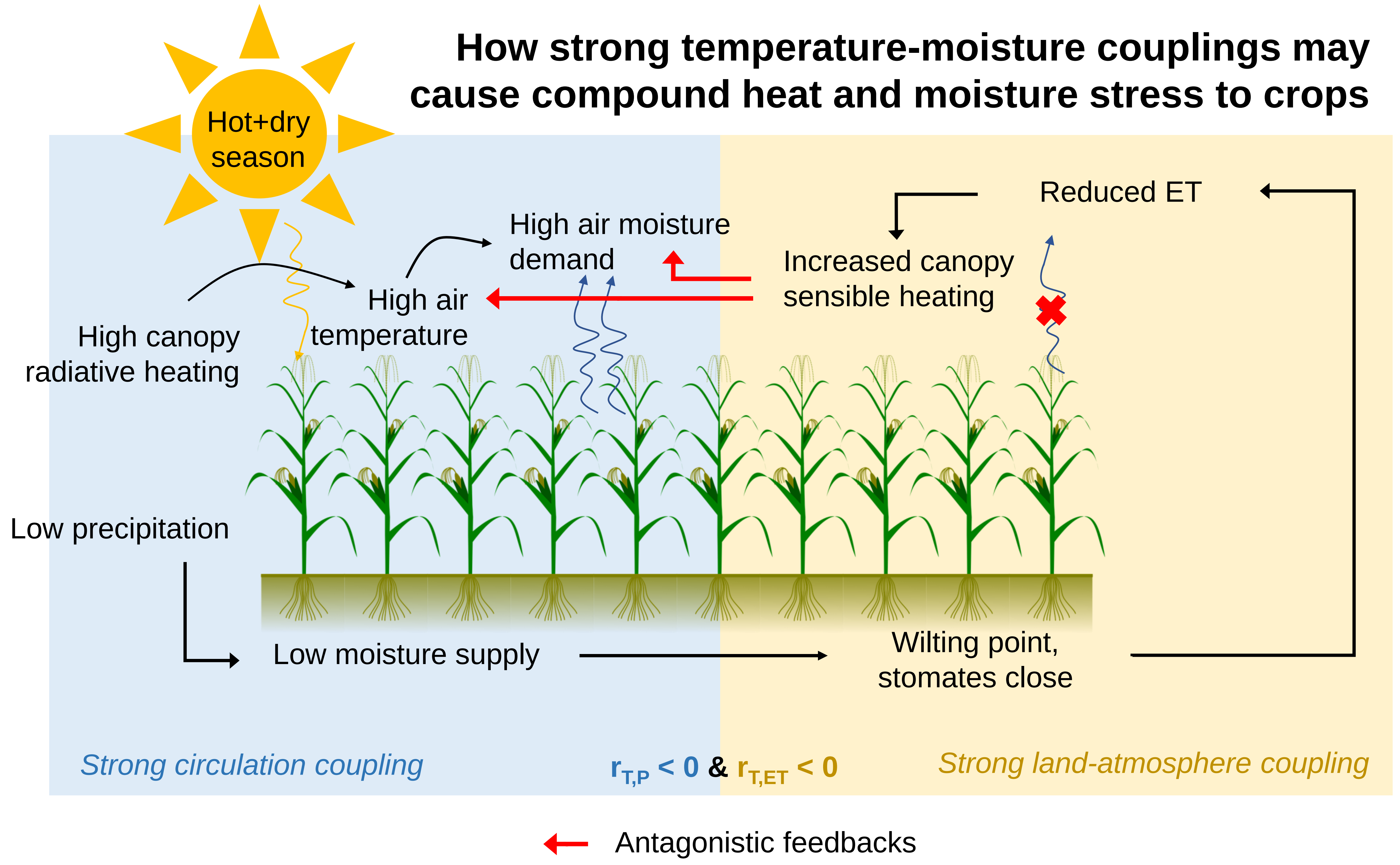
How strong temperature-moisture couplings may cause compound heat and moisture stress to crops
Hot+dry season
High air moisture demand
Reduced ET
Increased canopy sensible heating
High air temperature
High canopy radiative heating
Low precipitation
Low moisture supply
Wilting point, stomates close
Strong circulation coupling
$r_{T,P} < 0$ & $r_{T,ET} < 0$
Strong land-atmosphere coupling
Antagonistic feedbacks

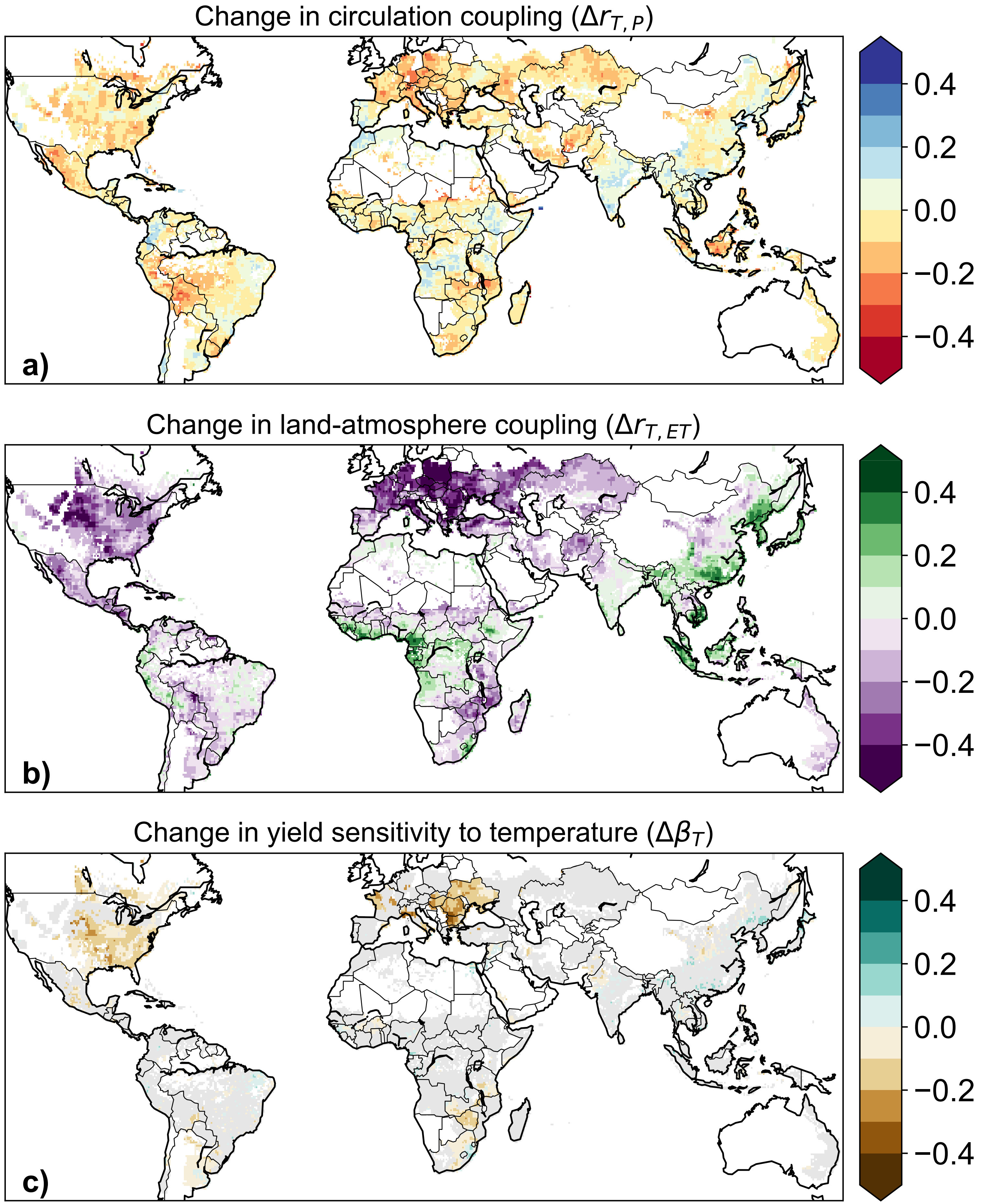

Change in circulation coupling ($\Delta r_{T,P}$)
0.4
0.2
0.0
−0.2
−0.4
a)
Change in land-atmosphere coupling ($\Delta r_{T,ET}$)
0.4
0.2
0.0
−0.2
−0.4
b)
Change in yield sensitivity to temperature ($\Delta\beta_T$)
0.4
0.2
0.0
−0.2
−0.4
c)

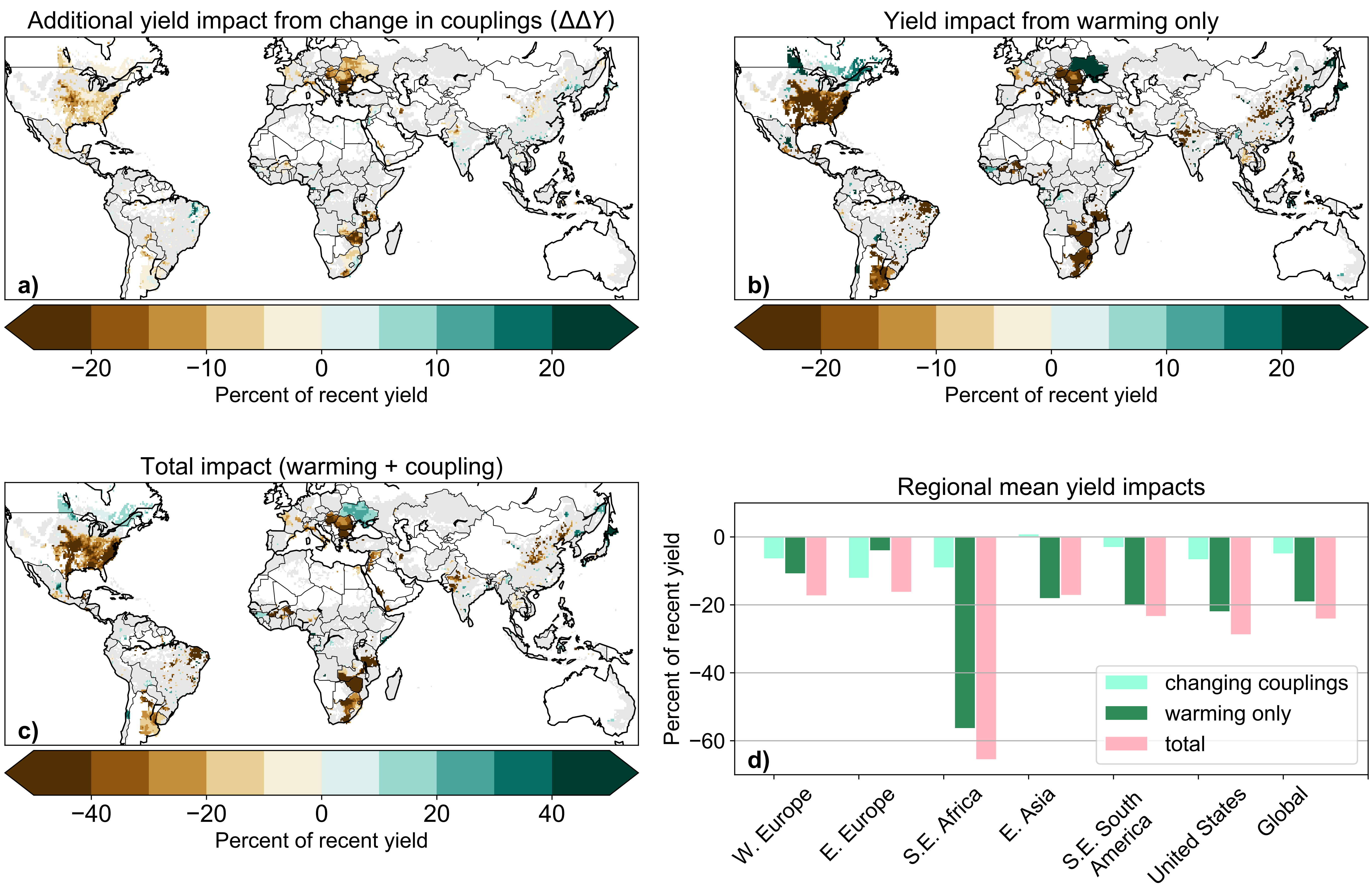
Additional yield impact from change in couplings (ΔΔY)
a)
−20
−10
0
10
20
Percent of recent yield
Yield impact from warming only
b)
−20
−10
0
10
20
Percent of recent yield
Total impact (warming + coupling)
c)
−40
−20
0
20
40
Percent of recent yield
Regional mean yield impacts
d)
Percent of recent yield
0
−20
−40
−60
changing couplings
warming only
total
W. Europe
E. Europe
S.E. Africa
E. Asia
S.E. South America
United States
Global

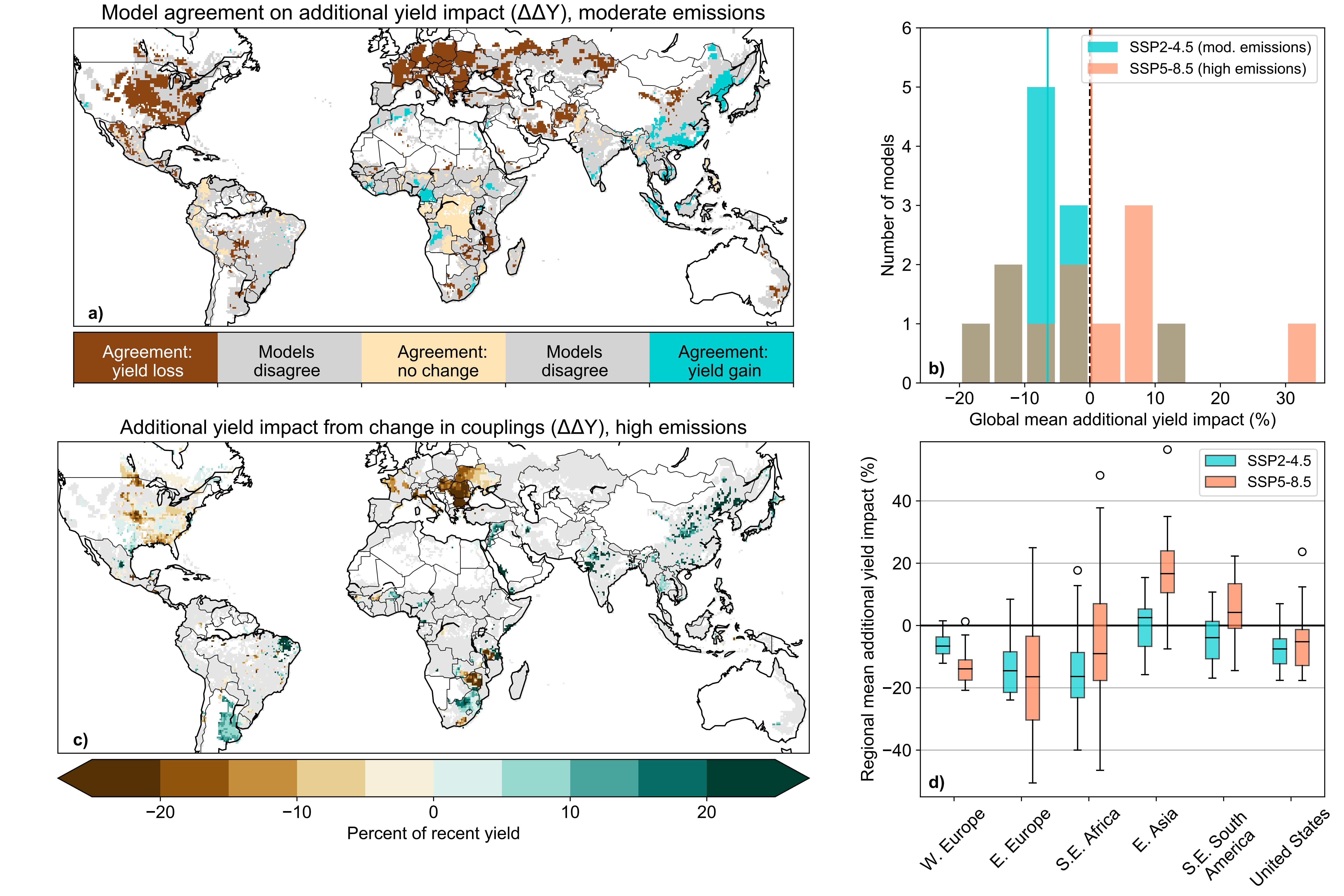

Model agreement on additional yield impact (ΔΔY), moderate emissions
a)
Agreement: yield loss
Models disagree
Agreement: no change
Models disagree
Agreement: yield gain
b)
SSP2-4.5 (mod. emissions)
SSP5-8.5 (high emissions)
Number of models
Global mean additional yield impact (%)
−20
−10
0
10
20
30
Additional yield impact from change in couplings (ΔΔY), high emissions
c)
Percent of recent yield
d)
SSP2-4.5
SSP5-8.5
Regional mean additional yield impact (%)
40
20
0
−20
−40
W. Europe
E. Europe
S.E. Africa
E. Asia
S.E. South America
United States